[Chem. Pharm. Bull. 33(6)2452—2460(1985)]

Dissolution Profiles of Nalidixic Acid Powders Having Weibull Particle Size Distribution

SHOZO KOUCHIWA,[a] MASAMI NEMOTO,[a] SHIGERU ITAI,*,[a]
HIROSHI MURAYAMA[a] and TSUNEJI NAGAI[b]

Research Laboratory, Taisho Pharmaceutical Co., Ltd.,[a] Yoshino-cho 1–403, Omiya, Saitama 330, Japan and Faculty of Pharmaceutical Science, Hoshi University,[b] Ebara 2–4–41, Shinagawa-ku, Tokyo 142, Japan

(Received August 21, 1984)

General equations were derived describing the exact dissolution profile and particle number reduction rate for powders of Weibull particle size distribution under sink conditions.

Several nalidixic acid (NA) powders of Weibull distribution, having mean diameter (μ), smallest diameter (r_0), and largest diameter (R_0) values of 400, 0, and 1000 μm respectively, were prepared by varying the parameters of the Weibull distribution. By means of dissolution tests of these powders, the effects of size distribution and truncation of powders having the same mean diameters were investigated. The results of the dissolution tests were consistent with those obtained in computer simulations, so that the derived equations were assumed to be reasonable.

The dissolution rate of powders of Weibull distribution, having the same mean diameter, increased as the size distribution became narrower. Upper-end truncation had more effect on the dissolution profile of the powders than lower-end truncation.

Keywords——dissolution profile; Weibull size distribution; truncated distribution; exact deviation; sink condition; computer simulation; nalidixic acid

Several investigations[1–7] have dealt with the problem of exactly describing the dissolution profile of powders in relation to the initial particle distribution under sink conditions. Most of these reports, however, have been restricted to powders initially consisting of particles with a log-normal distribution. In the present paper, the Weibull distribution was adopted to describe the initial particle size distribution. The effect of truncation on the dissolution profiles was then investigated both theoretically and experimentally.

Theoretical

The Dissolution Rate Equations in Relation to Initial Particle Size Distribution

Consider that the initial particle size distribution ($f_0(X_0)$) is transformed into $h(X)$ at time t in the dissolution process. Let the undissolved amount of the powder at time t (W) be expressed as:

$$W = N_t \cdot \int_0^\infty w(X,t) \cdot h(X)\,dX \tag{1}$$

where N_t is the number of particles remaining at time t, $w(X,t)$ is the weight of particles of diameter X at time t and the integrated portion is considered to be the mean particle weight at time t. Similarly, the initial amount of the powder (W_0) can be described as:

$$W_0 = N_0 \cdot \int_0^\infty w_0(X_0) \cdot f_0(X_0)\,dX_0 \tag{2}$$

where N_0 is the initial number of particles, and $w_0(X_0)$ is the initial weight of particles of diameter X_0. From Eqs. 1 and 2, the dissolved ratio at time t (Y) is given as:

$$Y=1-N_t\cdot\int_0^{\infty} w(X,t)\cdot h(X)\,dX\Big/\left\{N_0\cdot\int_0^{\infty} w(X_0)\cdot f_0(X_0)\,dX_0\right\} \tag{3}$$

In general, since the particle distribution is finite and has a maximum and a minimum, Eq. 3 can be rewritten as:

$$Y=1-N_t\cdot\int_{R_1}^{R_2} w(X,t)\cdot h(X)\,dX\cdot\int_{r_0}^{R_0} f_0(X_0)\,dX_0\Big/\left\{N_0\cdot\int_{r_0}^{R_0} w(X_0)\cdot f_0(X_0)\,dX_0\cdot\int_{R_1}^{R_2} h(X)\,dX\right\} \tag{4}$$

where R_1 and R_2 denote the diameter of the smallest and largest particle at time t, and r_0 and R_0 denote the initial diameter of the smallest and largest particle, respectively. If it is assumed that spherical particles dissolve isotropically under sink conditions and the solubility C_s is independent of particle size, the diameter X of a particle at time t is described by:[3)]

$$X=X_0-(2\cdot k\cdot C_s/\rho)\cdot t=X_0-K\cdot t \tag{5}$$

where k is the rate constant per unit area and ρ is the particle density. Then $w_0(X_0)$ and $w(X,t)$ of a spherical powder can be written as:

$$w_0(X_0)=(\pi\cdot\rho/6)\cdot x_0^3 \tag{6}$$

$$w(X,t)=(\pi\cdot\rho/6)\cdot(X_0-K\cdot t)^3 \tag{7}$$

In such cases, the diameter is reduced linearly as the dissolution proceeds so that K is considered to be the particle size reduction rate constant. Furthermore, the distribution pattern moves toward the smaller particle side without altering its shape, and at the time of X_0/K, the particles with initial size X_0 disappears. The function of the particle size distribution at time t ($h(X)$) is equal to that at initial time ($f_0(X_0)$), and then the particle number reduction ratio (N_t/N_0) can be written as:

$$N_t/N_0=\int_{R'_1}^{R'_2} f_0(X_0)\,dX_0\Big/\int_{r_0}^{R_0} f_0(X_0)\,dX_0 \tag{8}$$

where R'_1 and R'_2 denote the initial diameter of the smallest and the largest particles at time t and can be written as:

$$R'_1=r_0,\quad R'_2=R_0 \qquad \text{for} \quad t<r_0/K$$

$$R'_1=K\cdot t,\quad R'_2=R_0 \qquad \text{for} \quad r_0/K\leqq t<R_0/K$$

$$R'_1=R_0,\quad R'_2=R_0 \qquad \text{for} \quad t\geqq R_0/K$$

Furthermore, from substitution of Eqs. 6, 7 and 8 into Eq. 4, the general dissolution rate in relation to the initial particle distribution can be described by the following equation:

$$Y=1-\int_{R'_1}^{R'_2}(X_0-K\cdot t)^3\cdot f_0(X_0)\,dX_0\Big/\int_{r_0}^{R_0} X_0^3\cdot f_0(X_0)\,dX_0 \tag{9}$$

Adoption of the Weibull Distribution

The probability function of Weibull distribution is given by:

$$f_0(X_0)=b/a\cdot X_0^{b-1}\cdot\exp\{-(X_0^b/a)\} \tag{10}$$

where a is the scale parameter and b is the shape parameter. By use of these parameters, the peak point (R_{max}) and the mean diameter (μ) of powders of Weibull distribution are defined by the following equations:[8)]

$$R_{max}=\sqrt[b]{a(b-1)/b} \tag{11}$$

$$\mu=\int_{r_0}^{R_0} X_0\cdot f_0(X_0)\,dX_0 \Big/ \int_{r_0}^{R_0} f_0(X_0)\,dX_0$$

$$=\int_{r_0}^{R_0} X_0^b\cdot\exp\{-(X_0^b/a)\}dX_0/[\exp\{-(r_0^b/a)\}-\exp\{-(R_0^b/a)\}] \tag{12}$$

Furthermore, from substitution of Eq. 10 into Eqs. 8 and 9, the particle number reduction rate (N_t/N_0) and the dissolution rate (Y) of the powders of Weibull distribution are given by:

$$N_t/N_0=[\exp\{-(R'^b_1/a)\}-\exp\{-(R'^b_2/a)\}]/[\exp\{-(r_0^b/a)\}-\exp\{-(R_0^b/a)\}] \tag{13}$$

$$Y=1-\int_{R'_1}^{R'_2}(X_0-K\cdot t)^3\cdot X_0^{b-1}\cdot\exp\{-(X_0^b/a)\}\,dX_0 \Big/ \int_{r_0}^{R_0} X_0^{b+2}\cdot\exp\{-(X_0^b/a)\}\,dX_0 \tag{14}$$

Experimental

Material——NA and Polysorbate 80 were of JP X grade. All other chemicals were of reagent grade. Different particle size grades of NA were obtained by passing the material through Japan Industrial Standard (JIS) sieves and washing the product with 10^{-2}% (w/v) Polysorbate 80 solution saturated with NA.[9] A scanning electron photomicrograph of an NA particle is shown in Fig. 1.

The mean diameter of the sieved sample was calculated from the following equation:

$$R_m=\sqrt[3]{(6\cdot W_0)/(\pi\cdot\rho\cdot N_0)} \tag{15}$$

where N_0 of the sieved sample can be determined by counting the particle number in a samples of powder, and ρ was determined by use of a pycnometer (Beckman K.K.). The value of ρ was 1.50×10^{-9} mg/μm^3. N_0 and R_m of each sieved sample are shown in Table I.

Preparation of NA Powders of Weibull Distribution——The ratio of the number of particles in the size range from X_1 and X_2 to the total particle number is written as:

$$P=b/a\int_{X_1}^{X_2} X_0^{b-1}\cdot\exp\{-(X_0^b/a)\}\,dX_0 \Big/ \left[b/a\int_{r_0}^{R_0} X_0^{b-1}\cdot\exp\{-(X_0^b/a)\}\,dX_0\right]$$

$$=[\exp\{-(X_1^b/a)\}-\exp\{-(X_2^b/a)\}]/[\exp\{-(r_0^b/a)\}-\exp\{-(R_0^b/a)\}] \tag{16}$$

The ratio of the weight of particles in the size range from X_1 to X_2, to the total weight of the distributed powders can then be given by:

$$P_{wi}=P\cdot R_{mi}^3 \Big/ \sum_i P_i\cdot R_{mi}^3 \tag{17}$$

Based on Eqs. 16 and 17, two NA powders of Weibull distribution, with a mean diameter of 400 μm were prepared under the conditions of $b=2$ and $b=6$. Furthermore, a powder truncated at the upper end and a powder truncated at the lower end were also prepared. The particle size distribution (P) and the weight distribution (P_w) of the NA powders are shown in Table II.

Dissolution Study——Dissolution of the NA powders obtained by sieving through standard sieves and NA powders of Weibull distribution was tested in a USP dissolution test apparatus by using Method II: NA powder (50 mg) in 50% (v/v) ethanolic phosphate buffer solution, pH 6.8, was agitated at 150 rpm at 37 °C. Two-milliliter samples of the solution were withdrawn at appropriate intervals through a membrane filter (pore diameter: 0.45 μm) and immediately diluted with 18 ml of the test medium. The absorbance was determined at 258 nm on a spectrophotometer and the NA concentration was calculated from the absorbance of a standard solution.

Results and Discussion

Computer Simulation of the Dissolution of Powders of Weibull Distribution

The effects of particle size distribution and truncation of the powders of Weibull

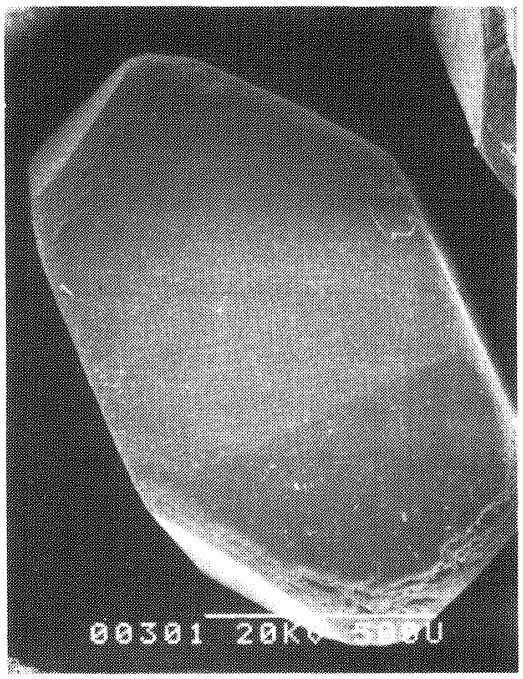

Fig. 1. Scanning Electron Photomicrograph of a Nalidixic Acid Particle (24—32 Mesh)

TABLE I. Values of Mean Diameter (R_m) of the Sieved Particles of Nalidixic Acid

Parameter	Mesh					
	16—20	20—24	24—32	32—48	48—60	60—80
W_0 (mg)	51.3	50.8	51.9	50.9	50.5	50.9
N_0	62	91	196	1.51×10^3	3.72×10^3	2.33×10^4 a)
R_m (μm)	1018	892	696	350	259	141

a) Determined by calculation from Eq. 20 under the condition of $K = 4.70\,\mu$m/min.

TABLE II. Preparations of Nalidixic Acid Powders of Weibull Distribution

Parameters			Powders of Weibull distribution (1)		(2)		(3)		(4)	
R_m (μm)	X_1 (μm)	X_2 (μm)	P (%)	P_w (%)	P (%)	P_w (%)	P (%)	P_w (%)	P (%)	P_w (%)
141	0	200	1.0	0.1	17.6	0.4	—	—	19.3	0.6
259	200	305	10.8	3.6	18.7	2.6	1.5	0.1	20.5	4.1
350	305	523	84.0	69.7	37.4	12.8	57.8	13.1	41.0	20.3
696	523	794	4.1	26.7	22.3	60.0	34.5	61.7	19.3	75.0
892	794	955	—	—	3.7	20.7	5.7	21.3	—	—
1018	955	1081	—	—	0.4	3.7	0.7	3.8	—	—
		Total	99.9	100.1	100.1	100.2	100.2	100.0	100.1	100.0

(1) $a = 6.40 \times 10^{15}$; $b = 6$; $r_0 = 0\,\mu$m; $R_0 = 1000\,\mu$m. (2) $a = 2.09 \times 10^5$; $b = 2$; $r_0 = 0\,\mu$m; $R_0 = 1000\,\mu$m. (3) $a = 2.09 \times 10^5$; $b = 2$; $r_0 = 300\,\mu$m; $R_0 = 1000\,\mu$m. (4) $a = 2.09 \times 10^5$; $b = 2$; $r_0 = 0\,\mu$m; $R_0 = 700\,\mu$m.

distribution were simulated on a microcomputer. From Eqs. 11 and 12, the a and R_{max} of the powders of Weibull distribution, the mean diameter (μ), the smallest particle diameter (r_0) and

TABLE III. Parameters of the Powders of Weibull Distribution ($\mu = 400\,\mu m$)

Parameters	Powders of Weibull distribution				
	A	B	C	D	E
a	2.09×10^5	8.99×10^7	3.79×10^{10}	1.57×10^{13}	6.40×10^{15}
b	2	3	4	5	6
R_{max} (μm)	323	391	411	417	418

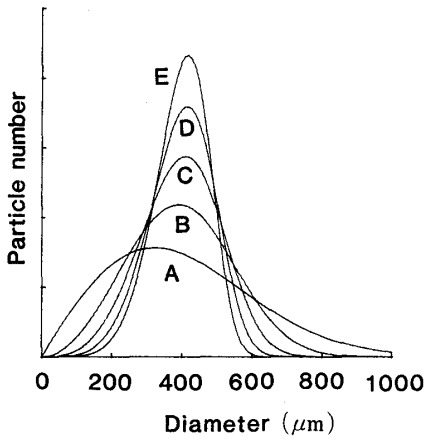

Fig. 2. Particle Size Distribution of the Powders of Weibull Distribution ($\mu = 400\,\mu m$)
A, $b=2$; B, $b=3$; C, $b=4$; D, $b=5$; E, $b=6$.

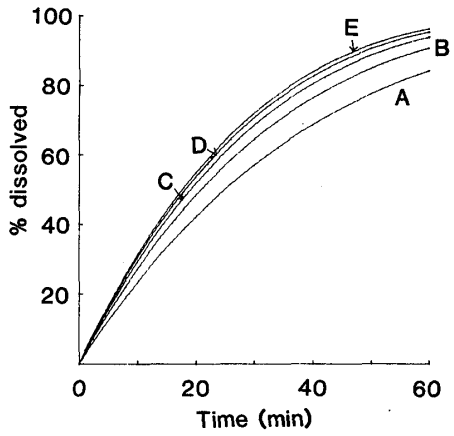

Fig. 3. Effect of Width of Distribution on the Dissolution Pattern of Particles
$r_0 = 0\,\mu m$; $R_0 = 1000\,\mu m$; $\mu = 400\,\mu m$; $K = 5\,\mu m/min$.
A, $b=2$; B, $b=3$; C, $b=4$; D, $b=5$; E, $b=6$.

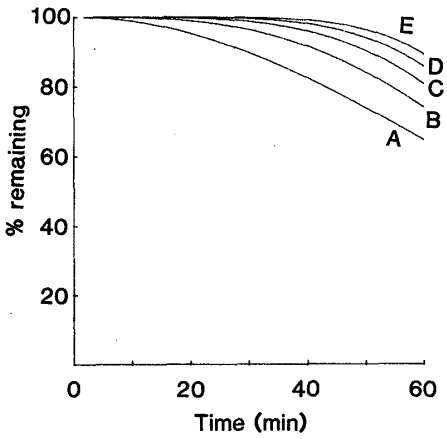

Fig. 4. Effect of Width of Distribution on the Particle Number Reduction Rate
$r_0 = 0\,\mu m$; $R_0 = 1000\,\mu m$; $\mu = 400\,\mu m$; $K = 5\,\mu m/min$.
A, $b=2$; B, $b=3$; C, $b=4$; D, $b=5$; E, $b=6$.

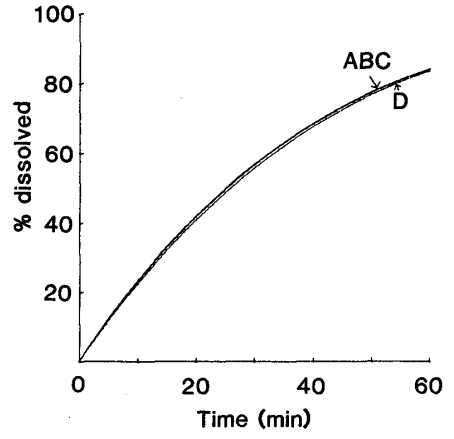

Fig. 5. Effect of Lower-End Truncation on the Dissolution Pattern of Particles
$a = 2.09 \times 10^5$; $b=2$; $R_0 = 1000\,\mu m$; $K = 5\,\mu m/min$.
A, $r_0 = 0\,\mu m$; B, $r_0 = 100\,\mu m$; C, $r_0 = 200\,\mu m$; D, $r_0 = 300\,\mu m$.

the largest particle diameter (R_0) of which were 400, 0, and 1000 μm, respectively, were calculated for $b=2$, 3, 4, 5 and 6. The results are shown in Table III and the particle size distribution patterns are shown in Fig. 2. The integrated portion of Eq. 12 as well as that of Eq. 14 was determined by Simpson's approximate integration, given by:

$$S=\int_{X_0}^{X_{2n}} y\mathrm{d}x=h/3\cdot\left\{(y_0+y_{2n})+4\sum_{k=1}^{n} y_{2k-1}+2\sum_{k=1}^{n-1} y_{2k}\right\} \tag{18}$$

$$h=(x_{2n}-x_0)/(2n) \tag{19}$$

The size distribution became narrower and R_{max} became larger as the parameter b increased. The dissolution patterns, as calculated from Eq. 14, for the powders in Fig. 2 with $K=5\,\mu$m/min are shown in Fig. 3. Although the mean diameters of the powders were equal ($\mu=400\,\mu$m), the dissolution rate was faster as the size distribution became narrower. The particle number reduction rate, as calculated from Eq. 13, for the powders of Weibull distribution in Fig. 2 with $K=5\,\mu$m/min are shown in Fig. 4. The reduction rate was slower as the size distribution became narrower.

The effects of truncation on the dissolution profile of the powders having $a=2.09\times10^5$ and $b=2$ are shown in Figs. 5 and 6. Comparison of the two figures indicates that the effect of truncation at the low end (Fig. 5) is very small and considerably less than that of truncation

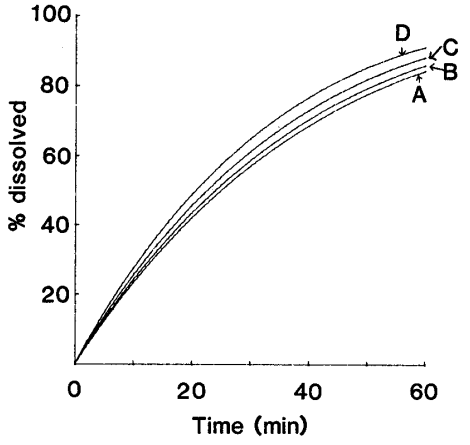

Fig. 6. Effect of Upper-End Truncation on the Dissolution Pattern of Particles

$a=2.09\times10^5$; $b=2$; $r_0=0\,\mu$m; $K=5\,\mu$m/min. A, $R_0=700\,\mu$m; B, $R_0=800\,\mu$m; C, $R_0=900\,\mu$m; D, $R_0=1000\,\mu$m.

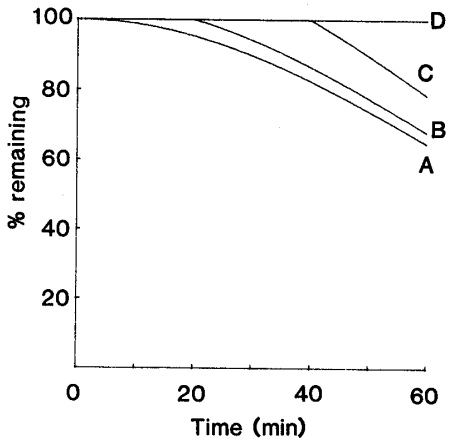

Fig. 7. Effect of Lower-End Truncation on the Particle Number Reduction Rate

$a=2.09\times10^5$; $b=2$; $R_0=1000\,\mu$m; $K=5\,\mu$m/min. A, $r_0=0\,\mu$m; B, $r_0=100\,\mu$m; C, $r_0=200\,\mu$m; D, $r_0=300\,\mu$m.

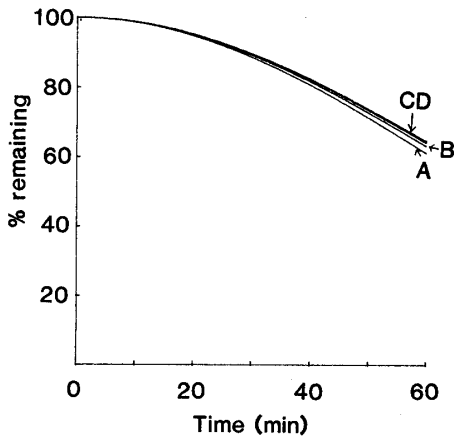

Fig. 8. Effect of Upper-End Truncation on the Particle Number Reduction Rate

$a=2.09\times10^5$; $b=2$; $r_0=0\,\mu$m; $K=5\,\mu$m/min. A, $R_0=700\,\mu$m; B, $R_0=800\,\mu$m; C, $R_0=900\,\mu$m; D, $R_0=1000\,\mu$m.

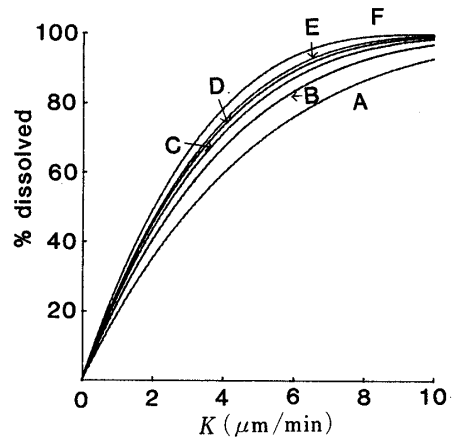

Fig. 9. Effect of K on the Dissolution Rate ($t=40$ min)

$r_0=0\,\mu$m; $R_0=1000\,\mu$m; $\mu=400\,\mu$m. A, $b=2$; B, $b=3$; C, $b=4$; D, $b=5$; E, $b=6$; F, monodisperse particles.

TABLE IV. Mean Diameter (μ) of the Truncated Weibull-Distributed Powders

Parameters	Upper-end-truncated powders (Fig. 6)				Lower-end-truncated powders (Fig. 5)		
	A	B	C	D	B	C	D
r_0 (μm)	0	0	0	0	100	200	300
R_0 (μm)	700	800	900	1000	1000	1000	1000
μ (μm)	360	380	392	399	416	457	513

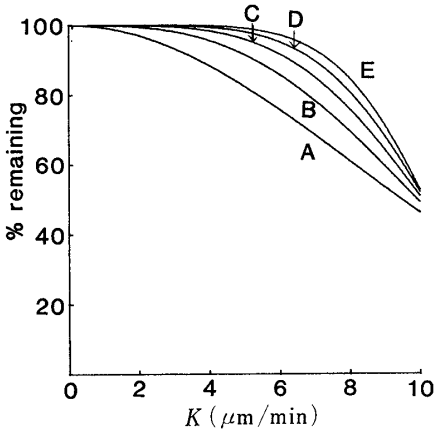

Fig. 10. Effect of K on the Particle Number Reduction Rate ($t=40$ min)

$r_0=0$ μm; $R_0=1000$ μm; $\mu=400$ μm. A, $b=2$; B, $b=3$; C, $b=4$; D, $b=5$; E, $b=6$.

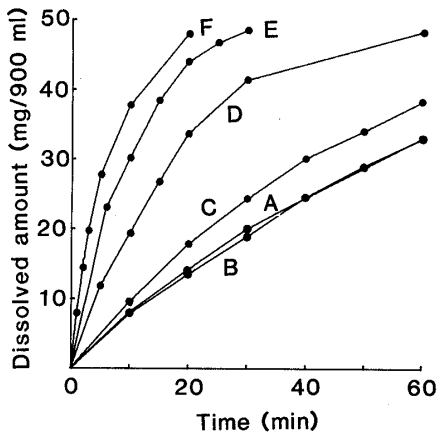

Fig. 11. Dissolution Rate of Nalidixic Acid ($W_0 \doteqdot 50$ mg)

A, 16—20 mesh; B, 20—24 mesh; C, 24—32 mesh; D, 32—48 mesh; E, 48—60 mesh; F, 60—80 mesh.

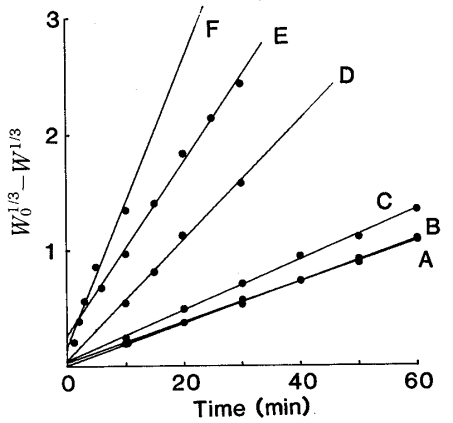

Fig. 12. Relationship between $W_0^{1/3}-W^{1/3}$ and Time for the Dissolution of Nalidixic Acid

A, 16—20 mesh; B, 20—24 mesh; C, 24—32 mesh; D, 32—48 mesh; E, 48—60 mesh; F, 60—80 mesh.

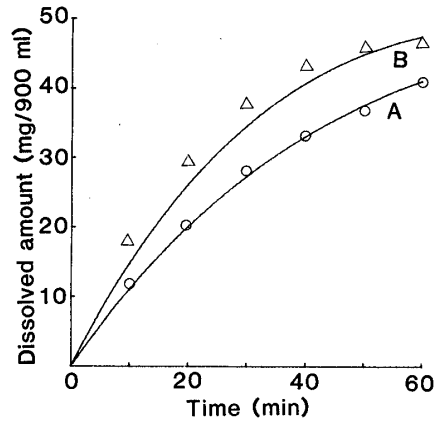

Fig. 13. Effect of Width of Distribution on the Dissolution Pattern of Nalidixic Acid

$r_0=0$ μm; $R_0=1000$ μm; $\mu=400$ μm; $K=4.70$ μm/min. A, $a=2.09\times10^5$, $b=2$; B, $a=6.4\times10^{15}$, $b=6$.

The symbols (○, $b=2$; △, $b=6$) are experimental data and the full lines are theoretical curves calculated from Eq. 14.

at the upper end (Fig. 6), as was found in log-normally distributed powders.[6] On the other hand, the particle number reduction patterns shown in Figs. 7 and 8 indicate that the effect of truncation at the upper end (Fig. 8) is very small and considerably less than that of truncation at the lower end (Fig. 7). The mean diameters (μ) of these truncated powders calculared from

TABLE V. Particle Size Reduction Rate (K) of the Sieved Particles of Nalidixic Acid

Parameters	Mesh					
	16—20	20—24	24—32	32—48	48—60	60—80
Slope	1.77×10^{-2}	1.84×10^{-2}	2.23×10^{-2}	5.21×10^{-2}	7.33×10^{-2}	1.24×10^{-1}
y-Intercept	2.19×10^{-2}	-4.13×10^{-3}	5.42×10^{-2}	3.70×10^{-2}	2.64×10^{-1}	1.47×10^{-1}
$r^{a)}$	0.999	0.999	0.999	0.999	0.997	0.990
K (μm/min)	4.84	4.43	4.16	4.92	5.12	4.70

a) Correlation coefficient.

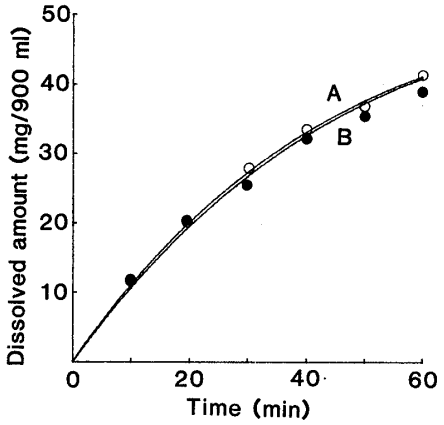

Fig. 14. Effect of Lower-End Truncation on the Dissolution Pattern of Nalidixic Acid

$R_0=1000\,\mu$m; $a=2.09\times10^5$; $b=2$; $K=4.70$ μm/min.
The symbols (○, $r_0=0\,\mu$m; ●, $r_0=300\,\mu$m) are experimental data and the full lines are theoretical curves calculated from Eq. 14 (A, $r_0=0\,\mu$m; B, $r_0=300\,\mu$m).

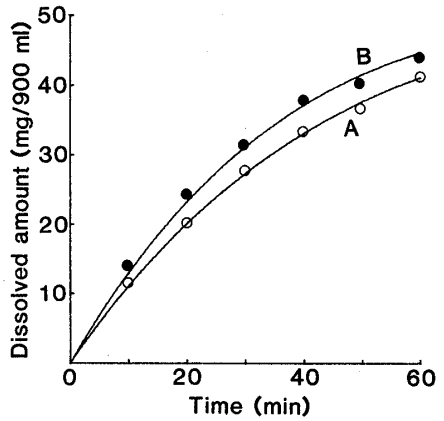

Fig. 15. Effect of Upper-End Truncation on the Dissolution Pattern of Nalidixic Acid

$r_0=0\,\mu$m; $a=2.09\times10^5$; $b=2$; $K=4.70\,\mu$m/min.
The symbols (●, $R_0=700\,\mu$m; ○, $R_0=1000\,\mu$m) are experimental data and the full lines are theoretical curves calculated from Eq. 14 (A, $R_0=1000\,\mu$m; B, $R_0=700\,\mu$m).

Eq. 12 are shown in Table IV.

The effect of the particle size reduction rate constant (K) on the dissolution rate and particle number reduction rate of powders in Table III at $t=40$ min are shown in Figs. 9 and 10, respectively. K seems to be a significant factor in determining the dissolution rate and particle number reduction rate.

Determination of K of Nalidixic Acid (NA)

The result of the dissolution test on NA powders passed through a series of standard sieves is shown in Fig. 11.

The rate of dissolution of the NA powders increased as the particle size was reduced. If the diameters of the sieved powders are considered to be the same, the following equation is obtained from Eqs. 6 and 7:

$$W_0^{1/3}-W^{1/3}=\{(\pi\cdot\rho\cdot N_0)/6\}^{1/3}\cdot K\cdot t \qquad (20)$$

where W_0 is the initial amount of powder and W is the undissolved amount of the powder at time t. Thus, plots of $W_0^{1/3}-W^{1/3}$ *vs.* t should be linear and from the slope of the line, K can be determined. The $W_0^{1/3}-W^{1/3}$ *vs.* t plots of NA powders are shown in Fig. 12. Each sieved powder showed a linear relation. The values of K for NA powders passed through a series of sieves ranging from 16 to 80 mesh, obtained by linear regression of the data in Fig. 12, are

shown in Table V. With powders whose particle sizes ranged from 16 to 60 mesh, K was almost constant so that the K of the NA powders was determined as an average ($K=4.70\,\mu$m/min).

Dissolution Profile of NA Powders

The results of the dissolution test of the NA powders listed in Table II are shown in Figs. 13—15. There is little difference between the experimental data and the theoretical data. From this dissolution study, the following conclusions were drawn both theoretically and experimentally.

(1) The dissolution rate of powders of Weibull distribution, which have the same mean diameter, increases as the size distribution becomes narrower.

(2) Upper-end truncation had a greater effect on the dissolution profile of the powders than lower-end truncation.

References

1) W. I. Higuchi and E. N. Hienstand, *J. Pharm. Sci.*, **52**, 67 (1963).
2) W. I. Higuchi, E. L. Rove and E. N. Hienstand, *J. Pharm. Sci.*, **52**, 162 (1963).
3) J. T. Carstensen and M. N. Musa, *J. Pharm. Sci.*, **61**, 223 (1972).
4) D. Brooke, *J. Pharm. Sci.*, **62**, 795 (1973).
5) D. Brooke, *J. Pharm. Sci.*, **63**, 344 (1974).
6) P. V. Pedersen and K. F. Brown, *J. Pharm. Sci.*, **64**, 1192 (1975).
7) N. Kitamori and K. Iga, *J. Pharm. Sci.*, **67**, 1674 (1978).
8) S. Kouchiwa, M. Nemoto, S. Itai, H. Murayama and T. Nagai, *Chem. Pharm. Bull.*, **33**, 1641 (1985).
9) N. Kaneniwa and N. Watari, *Chem. Pharm. Bull.*, **25**, 867 (1977).